Published in final edited form as:
Heart Rhythm. 2013 October ; 10(10): . doi:10.1016/j.hrthm.2013.07.020.

Heterogeneity and Function of K_{ATP} Channels in Canine Hearts

Hai Xia Zhang[1,2,*], **Jonathan R. Silva**[3,2,*], **Yu-Wen Lin**[1,2], **John W. Verbsky**[4,2], **Urvi S. Lee**[5], **Evelyn M. Kanter**[5], **Kathryn A. Yamada**[6], **Richard B. Schuessler**[5], and **Colin G. Nichols**[1,2]

[1]Department of Cell Biology and Physiology, Washington University School of Medicine, St. Louis, MO 63110, USA.

[2]Center for the Investigation of Membrane Excitability Diseases, Washington University School of Medicine, St. Louis, MO 63110, USA.

[3]Department of Biomedical Engineering, Washington University School of Medicine, St. Louis, MO 63110, USA.

[4]Department of Medicine, Washington University School of Medicine, St. Louis, MO 63110, USA.

[5]Department of Surgery, Washington University School of Medicine, St. Louis, MO 63110, USA.

[6]Mouse Cardiovascular Phenotyping Core, Washington University School of Medicine, St. Louis, MO 63110, USA.

Abstract

Background—The concept that pore-forming Kir6.2 and regulatory SUR2A subunits form cardiac ATP-sensitive potassium (K_{ATP}) channels is challenged by recent reports that SUR1 is predominant in mouse atrial K_{ATP} channels.

Objective—To assess SUR subunit composition of K_{ATP} channels and consequence of K_{ATP} activation for action potential duration (APD) in dog heart.

Methods—Patch-clamp techniques were used on isolated dog cardiomyocytes to investigate K_{ATP} channel properties. Dynamic current-clamp, by injection of a linear K^+ conductance to simulate activation of the native current, was employed to study consequences of K_{ATP} activation on APD.

Results—Metabolic inhibitor (MI)-activated current was not significantly different from pinacidil (SUR2A-specific)-activated current, and both currents were larger than diazoxide (SUR1- specific)-activated current, in both atrium and ventricle. Mean K_{ATP} conductance (activated by MI) did not differ significantly between chambers although, within the ventricle, both MI-induced and pinacidil-induced currents tended to decrease from epicardium to endocardium. Dynamic current-clamp results indicate that myocytes with longer baseline APDs are more susceptible to injected "K_{ATP}" current, a result reproduced *in silico* using a canine AP model to simulate Epi and Endo (HRd).

Corresponding author: Colin G. Nichols, PhD, Department of Cell Biology and Physiology, Box 8228, Washington University School of Medicine, 660 S. Euclid Ave., St. Louis, MO 63110, Ph: (314) 362-6630; Fax: (314) 362-7463, cnichols@wustl.edu.
*These authors contributed equally

Conflict of Interest Statement: The authors declare that they have no conflict of interest.

Conclusions—Even a small fraction of K_{ATP} activation significantly shortens APD in a manner that depends on existing heterogeneity in K_{ATP} current and APD.

Keywords

ATP sensitive potassium channel; sulfonylurea receptor; patch-clamp technique; action potential duration; pinacidil; diazoxide; metabolic inhibition; model simulation; canine; myocyte

INTRODUCTION

K_{ATP} channels are formed by four pore-forming subunits (Kir6.1 or Kir6.2) and four regulatory sulfonylurea receptors (SUR1, SUR2A, or SUR2B)[1]. SUR subunits cause channel opening when bound to MgADP or channel openers (eg, pinacidil and diazoxide), and transduce channel inhibition by sulfonylureas (eg, glibenclamide and tolbutamide). Different combinations of expressed subunits result in qualitative and quantitative differences in functional properties in specific tissues. For example, in the pancreas, the Kir6.2/SUR1 complex regulates insulin secretion in response to glucose-dependent changes in metabolism[2]. Conversely cardiac K_{ATP} channels contain Kir6.2 and SUR2A subunits[3], which are less responsive to nucleotide activation than SUR1-containing channels[4] and remain predominantly closed under physiological conditions[5], explaining lack of cardiac abnormalities in patients with **neonatal diabetes or** hyperinsulinism due to Kir6.2-dependent K_{ATP} mutations. However, recent studies reveal that cardiac K_{ATP} channels in mice differ in a chamber-specific fashion: Kir6.1-containing channels may be prominent in conduction system myocytes[6], and in particular, atrial K_{ATP} channels are formed by SUR1/Kir6.2 while ventricular channels contain SUR2A/Kir6.2[7].

Even moderate K_{ATP} channel opening can cause dramatic action potential (AP) shortening[8–10]. As a consequence of higher sensitivity to activation by intracellular nucleoside diphosphates[4], cardiac SUR1 expression could therefore implicate K_{ATP} channel participation in cardiac excitation under nominally physiological conditions; recent studies have found that cardiac K_{ATP} channels may open during strenuous exercise[11] and stress[12]. On one hand, AP shortening due to K_{ATP} channel opening may provide cardioprotection by reducing contractile force and energy consumption in response to ischemia or other stresses. On the other hand, K_{ATP} channel opening might predispose to arrhythmias due to AP shortening, external potassium accumulation, and dispersion of transmural repolarization, particularly if localized regions of the heart respond differentially. Because K_{ATP} activation depends on channel composition, differential K_{ATP} channel subunit expression may lead to distinct consequences of K_{ATP} activation throughout the heart, such as chamber-specific response to ischemia or other stresses[13]. To date, potential subunit heterogeneity in large animals is unexplored. In the present study, we performed a detailed examination of the regional heterogeneity of canine cardiac sarcolemmal K_{ATP} pharmacology, as well as the consequences of heterogeneous cellular responses by injecting simulated K^+ current into native myocytes via dynamic clamp.

METHODS

Cardiomyocyte isolation

All protocols were approved by the Animal Studies Committee at Washington University School of Medicine. Hearts were harvested from 9–12 month old mongrel canines (7 males, 10 females) weighing 19–30 kg. All animals were anesthetized with intravenous propofol (7 mg/kg), intubated with a cuffed endotracheal tube and mechanically ventilated with a pressure-controlled ventilator. An adequate level of anesthesia was maintained by inhaled

isoflurane (1%–3%) and a limb-lead ECG was monitored. After hypothermic cardioplegic arrest, the explanted heart was place in cold saline solution.

Atrial myocyte isolation

In cold saline solution, ventricular branches from the right coronary artery were ligated with silk sutures. The right coronary artery was cannulated at the right coronary cusps and perfused with 2 mM Ca^{2+}-Tyrode solution (in mM: 136 NaCl, 5.4 KCl, 2 $CaCl_2$, 1 $MgCl_2$, 0.33 NaH_2PO_4, 5 HEPES, 10 glucose, pH 7.35). The tissue was digested by perfusing the following solutions at 40 mL/min at 37°C: 2 mM Ca^{2+}-Tyrode's for 10 min, Ca^{2+}- free Tyrode's for 10 min, and 0.05% collagenase + 0.1% Albumin in Ca^{2+} free Tyrode's for 60 min, while bubbling with 100% O_2. After digestion, the tissue lateral to the crista terminalis was excised and gently triturated to tease apart the tissue and to suspend isolated myocytes cells in 200 μM Ca^{2+}-Tyrode's solution.

Ventricular myocyte isolation

After the right atrium was removed, the remainder of the heart was immediately transferred to cold, oxygenated Ca^{2+}-free modified Krebs solution (in mM; 118 NaCl, 4.8 KCl, 1.2 $MgCl_2$, 11 glucose, 1.2 KH_2PO_4, 25 $NaHCO_3$, 0.03 EGTA, 1× MEM amino acids, 1.5 nM insulin, pH 7.30), and a branch of the left anterior descending artery was cannulated, to start perfusion with a syringe. Cannulated tissue was then attached to perfusion tubing and maintained at 37°C in an incubator. Tissue was perfused with Ca^{2+}-free modified Krebs solution for 15 min and 0.08% collagenase solution (200 U/ml collagenase in 35 μM Ca^{+} modified Krebs solution) for another 15 min. Epicardial (Epi) and endocardial (Endo) surfaces were separated from mid-myocardium (Mid) and transferred to individual petri dishes, each with 20 ml 0.08% collagenase solution. These tissue sections were gently chopped into small pieces, and incubated in a shaking bath for 10 min at 37° and 80 rpm. After incubation, the supernatant was discarded, and 20 ml 0.08% collagenase solution was added to each flask for 15 min. The supernatant was then collected and filtered and additional collagenase solution was added for a further 15 min. This process was repeated and supernatants acquired from all three incubations. Supernatants were centrifuged at 45 × g for 2 min and myocytes were re-suspended in 50 μM Ca^{2+}-HEPES solution (in mM; 133.5 NaCl, 4.8 KCl, 1.2 $MgCl_2$, 1.2 KH_2PO_4, 10 HEPES, 10 glucose, 0.05 $CaCl_2$, 10 taurine, 1× MEM amino acids, 0.5 pyruvate, 1.5 nM insulin, 0.5% BSA, pH 7.30).

Electrophysiological recordings

Cardiomyocytes were voltage- or current-clamped in whole-cell or excised patch mode using an Axopatch 200A amplifier (Molecular Devices, Sunnyvale, CA), and signals were digitized using a Digidata 1322A digitizer board (Molecular Devices, Sunnyvale, CA) after 4-pole low-pass Bessel filtering at 2 kHz. Signals were digitized at 10 kHz using pCLAMP 8 (Molecular Devices, Sunnyvale, CA) and analyzed using pCLAMP 9 software (Molecular Devices, Sunnyvale, CA).

Conventional whole-cell recording

Isolated myocytes were transferred to the recording chamber using a Pasteur pipette and continuously perfused at room temperature with extracellular solution containing (in mM): 137 NaCl, 5.4 KCl, 0.5 $MgCl_2$, 3 $NaHCO_3$, 0.2 NaH_2PO_4, 5 HEPES, 10 Glucose, pH 7.40. Electrodes had 1.5–2.0 MΩ resistance when filled with pipette solution (in mM): 130 K-aspartate, 20 KCl, 4 K_2HPO_4, 1 $MgCl_2$, 10 EGTA, 0.1 K_2ATP, and 10 HEPES, pH 7.20–7.30. K_{ATP} currents were activated by applying metabolic inhibitors (MI, 2 mM NaCN plus 10 mM Deoxyl-glucose replacing glucose), 100 μM pinacidil or 100 μM diazoxide to the bath solution (test solution). K_{ATP} currents were continuously assessed using a 4-s voltage

ramp from –120 mV to +40 mV from a holding potential of –70 mV. K_{ATP} current amplitude was typically measured at +40 mV, and reported conductances (used in simulations) were measured as the slope conductance between –75 to –65 mV.

Perforated whole-cell recording

Isolated myocytes were continuously perfused at 35–37°C with extracellular solution containing (in mM): 137 NaCl, 5.4 KCl, 1.5 $CaCl_2$, 0.5 $MgCl_2$, 3 $NaHCO_3$, 0.2 NaH_2PO_4, 5 HEPES, 10 Glucose, pH 7.40. Patch clamp electrodes were tip-filled with pipette solution (in mM: 110 K-asparate, 20 KCl, 1 $MgCl_2$, 0.5 $CaCl_2$, 5 EGTA, 5 K_2ATP, 10 HEPES, pH 7.2–7.3), and back-filled with the same pipette solution containing 250 μg/ml nystatin. Whole-cell configuration was typically achieved within 5 min after forming a gigaohm seal. To examine the physiological consequences of differential K_{ATP} expression, we used a dynamic clamp circuit (Fig. 1)[14] in which we injected a simulated K_{ATP} current (KATP-INJ) via an analog circuit (Fig. 1) to simulate a progressively increasing linear K^+ conductance. The analog circuit generated a voltage-independent conductance reversing at manually set E_K (–80 mV) that could be manually altered to apply currents up to 50 pA.

Excised inside-out patch-clamp recording

Pipettes had resistances of 1.0–1.5 MΩ when filled with ATP-free Kint (in mM, 140 KCl, 10 HEPES, 1 EGTA, 1 K_2-EDTA, and 4 K_2HPO_4, pH 7.40). Following forming of an on-cell gigaohm seal, the patch was excised and responses to various dugs examined as described. Patch current was recorded at a pipette potential of +50 mV at pipette potential, i.e. –50 mV membrane potential. Diazoxide or pinacidil-induced current was normalized as the percentage of ATP-free Kint current.

Simulations

Action potentials were simulated with the 2010 Hund-Rudy canine ventricular cell model[15]. To better match observed AP durations, the magnitudes of the repolarizing I_{Ks} and I_{Kr} conductances were increased to 220 and 380 pS/pF, respectively and the magnitude of the late Na^+ current was decreased to 1.3 pS/pF. To simulate shorter action potentials (<140 ms) I_{Ks} and I_{Kr} conductance magnitudes were further increased to 1240 and 2100 pS/pF, respectively. Sets of ordinary differential equations were solved with the forward Euler method and a fixed time step of 5 μs. Simulations were executed on a Beowulf cluster. Each node utilized 12, 2.3 GHz, Intel Xeon cores, allowing simulations to complete within minutes.

Statistics

Data are presented as the mean ± standard error of the mean (S.E.M.) with n (n = cell or patch number, heart number) being the number of cells and hearts in whole-cell recording or patches and hearts in excised patch recording. All data were first analyzed using a linear mixed model (SAS) with “heart” as a random effect to detect the significance of “heart” in all the measurements. The results show that the “heart” was not significant, so myocytes were treated as independent samples in the analysis. Statistical analysis was performed using a two-tailed student t-test, one-way ANOVA followed by Tukey’s *post hoc* comparison of means or two-way ANOVA followed by Bonferroni’s post-tests, as appropriate. Statistical significance was set as $p< 0.05$.

Materials

Collegenase was purchased from Worthington Biochemical Corporation (Lakewood, NJ). All other chemicals were obtained from Sigma (St. Louis, MO) unless indicated otherwise.

RESULTS

Atrial K_{ATP} channels are fully activated by pinacidil and slightly activated by diazoxide

After stable whole-cell patch-clamp configuration was achieved, the bath solution was switched to a test solution containing MI, diazoxide, or pinacidil (Fig. 2A), to assess K_{ATP} densities in atrial myocytes (cell capacitance 86 ± 7 pF, n = 19, 5). Pinacidil activates SUR2A-containing channels, while diazoxide activates channels that contain SUR1[16, 17]. Pinacidil-induced current (40 ± 4 pA/pF, n = 14, 5) did not significantly differ from MI-induced current (49 ± 9 pA/pF, n = 11, 5; Fig. 2B). Diazoxide induced a much smaller, but still significant K_{ATP} current (8 ± 5 pA/pF, n = 11, 5; P<0.05 by ANOVA, Fig. 2B). These results suggest that ~20% of dog atrial K_{ATP} channels may be regulated by SUR1, whereas almost all channels are regulated by SUR2A.

Ventricular K_{ATP} channels are predominantly pinacidil-activated

Ventricular K_{ATP} channel composition and heterogeneity was independently assessed in epicardial (Epi), mid-myocardial (Mid), and endocardial (Endo) myocytes. No statistical difference in capacitance was detected between myocytes from these regions (148 ± 25 pF in Epi, n = 9, 3; 102 ± 25 pF in Mid, n = 7, 3; and 139 ± 21 pF in Endo, n = 12, 4; p>0.05 by one-way ANOVA). Pinacidil-induced current was not significantly different from MI-induced current in Epi (62 ± 16 pA/pF, n = 5, 3; versus 53 ± 11 pA/pF, n = 7, 3; p>0.05), Mid (43 ± 11 pA/pF, n = 6, 3; versus 46 ± 10 pA/pF, n = 7, 3; p>0.05), or Endo (37 ± 7 pA/pF, n = 5, 4;versus 29 ± 5 pA/pF, n = 6, 4; p>0.05) myocytes, suggesting that SUR2A is also the predominant subunit across the ventricular wall (Fig. 3). Pinacidil-induced currents as well as MI-induced currents were non-significantly smaller in Endo than Epi and Mid (P>0.05 by two-way ANOVA), implying a weakly heterogeneous transmural K_{ATP} density across the ventricle. Consistently, diazoxide-induced current was negligible compared with MI- or Pinacidil-induced current in Epi (6 ± 5 pA/pF, p<0.05 by two-way ANOVA), Mid (1 ± 3 pA/pF, p<0.05 by two-way ANOVA), and Endo (2 ± 1 pA/pF, p<0.05 by two-way ANOVA) (Fig. 3).

Pinacidil induces K_{ATP} currents in excised atrial and ventricular membrane patches

K_{ATP} channel expression and drug sensitivities were also probed with excised inside-out patch recordings from right atrial (Fig. 4A), left ventricular Epi (Fig. 4B top), mid (Fig. 4B middle) and Endo (Fig. 4B bottom) myocyes. Consistent with larger pinacidil-induced whole-cell current, pinacidil-induced patch current (relative to current in zero ATP) was much greater than diazoxide-induced current in atrial myocytes (3.2 ± 1.0 pA versus 0.3 ± 0.08 pA, n = 10, 3; p<0.05 by t-test, Fig. 4A, C), as well as in ventricular Epi (1.8 ±0.7 pA versus 0.2 ±0.05 pA, n = 7, 2), Mid (2.1 ± 0.5 pA versus 0.08 ± 0.01 pA, n = 6, 2), and Endo (1.4 ± 0.5 pA versus 0.17 ± 0.06 pA, n = 5, 2) myocytes (P<0.05 by two-way ANOVA, Fig. 4B, C). In addition, pinacidil-induced patch current tended to be non-significantly smaller in Endo compared to Epi, and Mid.

Myocytes with longer APD are more sensitive to injected "K_{ATP} current"

We examined the physiological consequences of differential K_{ATP} expression by injecting simulated K_{ATP} current ($K_{ATP\text{-}INJ}$) via dynamic clamp (Fig. 1) [14] into atrial and ventricular myocytes under perforated whole-cell current-clamp (Fig. 5A). After normalizing for cell size, APD (averaged over twenty APs at a cycle length (CL) of 1000 ms), was plotted versus $K_{ATP\text{-}INJ}$ conductance, which ranged from 0 to 4 pS/pF (Fig. 5B, left). Starting APDs for individual cells (i.e. without injected current) are indicated by dashes on the right of each plot. Consistent with previous reports of high APD variability[18], we observed a large range with long APDs in myocytes from the Mid and Epi layers. As a group, Epi and Mid

myocytes showed relatively high sensitivity to $K_{ATP\text{-}INJ}$. In contrast, Endo and atrial myocytes were relatively resistant to $K_{ATP\text{-}INJ}$. Prior AP shortening, as a result of rapid pacing (CL = 300 ms), reduced the sensitivity to $K_{ATP\text{-}INJ}$ in Epi and Mid, while leaving Endo and right atrial APD relatively unaffected (Fig. 5B right). The level of $K_{ATP\text{-}INJ}$ necessary to cause a 50% reduction in APD was 1.00 ± 0.27 (n = 4, 1), 2.40 ± 0.62 (n = 4, 2), 2.03 ± 0.45 (n = 7, 2), and 3.25 ± 0.66 (n = 6, 2) pS/pF for Epi, Mid, Endo and RA, myocytes, respectively. These averages corresponded to 0.4 – 0.9% of the total K_{ATP} current in each region, consistent with previous estimates of the relative effectiveness of the available K_{ATP} conductance in ventricular myocytes from rat or guinea pig[14, 19].

The sensitivity of longer APs to injected K_{ATP} currents is illustrated in Fig. 5C. At a conductance of 3.5 pS/pF, myocytes with baseline APD >140 ms show ~70% shortening, whereas cells with APD <140 ms show only ~40% shortening (p = 0.02). In the same myocytes paced at CL = 300 ms, there is a modest decrease in sensitivity of longer APs, whereas shorter APs are unaffected, but the cells with longer APs still show greater shortening than those with shorter APs (p = 0.048).

To examine whether computational models could account for the observed behavior, increasing levels of K_{ATP} were simulated with the 2010 HRd canine ventricular AP model[15]. Longer APs were simulated by the starting conditions (APD of 195 ms), whereas shorter APs (APD of 96 ms) were obtained by increasing I_{Kr} and I_{Ks} conductances, as detailed in the Methods. Approximately 5× more injected K_{ATP} current is required to cause similar APD shortening in the model than is observed in experiments. This difference in sensitivity was not easily accounted for by varying the conductances of major currents (data not shown), suggesting that the kinetic parameters that describe the currents may be responsible. Nevertheless, the model does qualitatively reproduce differential sensitivity of short and long APs in addition to blunted effect of K_{ATP} at faster pacing rates (Fig. 5D).

DISCUSSION

Heterogeneity of cardiac K_{ATP} channels differs between species

SUR subunits, encoded by *ABCC8* (SUR1) and *ABCC9* (SUR2) [1] endow K_{ATP} channels with distinct sensitivity to K_{ATP} channel inhibitors and activators. The consensus notion that cardiac K_{ATP} channels are SUR2A-based[3, 20], is now questioned by studies that show inhomogeneous SUR distribution in mouse heart: SUR1 predominates in atria, SUR2A in the ventricles, and SUR2B may be expressed in the conduction system[6, 7]. The present results imply that the SUR distribution in larger hearts is less marked: both atrial and ventricular canine K_{ATP} appear to be primarily regulated by SUR2A subunits, but small diazoxide-induced currents in both atrial and ventricular myocytes imply the presence of SUR1-dependent channels at low levels. A similar SUR1 and SUR2A distribution seems likely in human atrium and ventricle[21]. Thus, in larger mammals, the distribution of SURx subunits may be predominantly SUR2A in all chambers, with low expression of SUR1 in both atria and ventricles. K_{ATP} expression levels may vary in different species and regions of the heart. Measured under the same conditions, K_{ATP} current density in mouse heart is between 100–600 pA/pF[24] but only 20–100 pA/pF in dog heart. These points should be carefully considered when using other species to model normal or diseased human hearts.

Studies from heterologous expression systems have shown that SUR1 and SUR2 subunit can coexist within a single functional K_{ATP} channel[22, 23] and heterogeneous SURx composition may also be the case in native K_{ATP}, since pinacidil and diazoxide both induce currents from the same cardiomyocytes and in the same excised patches. It has recently been shown that cardiac K_{ATP} channels provide protection during adaptation to physiological stress[11], which may imply a physiological role for opening of SUR1-based K_{ATP} channels, since SUR1

channels will open at higher ATP concentrations[4]. Deliberate overexpression of SUR1 together with a gain-of-function mutation of Kir6.2 in mice led to embryonic lethality and arrhythmias[25, 26].

Transmural heterogeneity and function of cardiac K_{ATP} channels

Ventricular myocytes are organized into three layers with distinct electrophysiological profiles: Epi, Mid and Endo[18, 27]. Epi and Mid tend to have a prominent notch in phase I due to larger I_{to}. Mid exhibit larger late I_{Na}, larger sodium-calcium exchange current ($I_{Na/Ca}$), and smaller I_{Ks}, leading to a longer APD. The present study suggests that heterogeneity of K_{ATP} current, as previously reported in feline Epi- versus Endo-mycoytes [28], may generate distinct pharmacologic profiles and responses to pathophysiologic states. Heterogeneity of AP shortening by K_{ATP} channel opening between epicardium and endocardium has been reported in canine ventricle[29]. The AP is preferentially shortened by pinacidil in epicardium[30], potentially due to the larger I_{to}-dependent AP notch, although larger epicardial K_{ATP} density might also contribute. Greater AP shortening due to K_{ATP} opening in epicardium could result in transmural dispersion of repolarization, causing ST-segment elevation and phase 2 reentry, precipitating ventricular tachycardia and ventricular fibrillation[29, 30] during ischemia. AP shortening caused by ischemia is more pronounced in the epicardium [28, 31], and the present results suggest that increased epicardial expression of K_{ATP} channels may in part be responsible.

In silico analysis using the HRd model confirmed that activation of a small fraction of available K_{ATP} channels can have dramatic effects on the cellular electrophysiology[19], although the model implies a weaker effect of K_{ATP} activation than demonstrated by current-injection experiments (Fig. 5C,D). While it is beyond the scope of this study to reformulate the model, these quantitative differences may lie in the description of $I_{Ca,L}$, whose activation may in reality be more susceptible to small increases in outward plateau current. Previous studies have shown proarrhythmic consequences when K_{ATP} is sufficiently activated to cause a loss of the dome in AP morphology, in myocytes that express high levels of I_{to} [30]. By applying our dynamic-clamp methodology to dissociated myocytes we observed enhanced sensitivity of myocytes with longer APD to simulated K_{ATP}. Greater fractional shortening in myocytes with long APDs is consistent with greater rate-adaptation of APD in mid-myocardial cells with prolonged APD[18], and with the concept of reduced "repolarization reserve" in which patients with previously compromised repolarizing currents are more susceptible to QT prolongation and arrhythmia when repolarizing currents are additionally blocked by drugs[32]. Physiologically, increased sensitivity of these cells to K_{ATP} activation would tend to result in enhanced APD uniformity across the ventricular wall, once activation is initiated. This effect on the overall dispersion of APD would likely persist until catastrophic loss of the dome, in a cell with increased I_{to}. In intact tissue, AP synchronization through gap junction-coupling may minimize the effect of K_{ATP} channel activation on AP uniformity, but K_{ATP} channels may provide a strong influence in diseased conditions where APD can show larger dispersion.

The influence of subtle heterogeneities of K_{ATP} density or properties on APD may be amplified under exercise or mild ischemia. Even if expressed at low levels, the higher sensitivity of SUR1- containing channels to nucleotide activation[4] could have dramatic consequences. Finally, we detected no major difference in K_{ATP} density between atrium and ventricle, yet even similar activation may have less effect in atrium due to the intrinsically shorter atrial APD. Previous studies have shown that interaction between I_{to} and K_{ATP} can induce a heterogenous response[30], but quantitative evaluation of K_{ATP} effects across the myocardium reveals complex dependence of the physiological response on composition of the channel, APD, and level of channel expression.

Acknowledgments

We thank Yefei Cai (Statistical data analyst, Department of Psychiatry, Washington University in St. Louis) for her help with the statistics.

This work was supported by a NIH grant (HL95010 to CGN) and a Burroughs Wellcome Fund Career Award at the Scientific Interface 1010299 (to JS). Tissue was harvested by the Translational Cardiovascular Biobank & Repository at Washington University, supported by NIH/CTSA grant UL1 TR000448.

Abbreviations

K_{ATP}	ATP sensitive potassium channel
AP	action potential
APD	action potential duration
EGTA	ethylene glycol-bis(2-aminoethylether)-N,N,N',N'-tetraacetic acid
HEPES	4-(2-hydroxyethyl)-1-piperazineethanesulfonic acid
MI	metabolic inhibitors
INa	sodium current
ICa,L	L-type Ca2+ current
Ito	transient outward current
IKs	slow delayed rectifier current
IKr	rapid delayed rectifier current
IK1	inward rectifier current.

REFERENCES

1. Nichols CG. Katp channels as molecular sensors of cellular metabolism. Nature. 2006; 440:470–476. [PubMed: 16554807]
2. Remedi MS, Nichols CG. Hyperinsulinism and diabetes: Genetic dissection of beta cell metabolism-excitation coupling in mice. Cell Metab. 2009; 10:442–453. [PubMed: 19945402]
3. Babenko AP, Gonzalez G, Aguilar-Bryan L, Bryan J. Reconstituted human cardiac katp channels: Functional identity with the native channels from the sarcolemma of human ventricular cells. Circ Res. 1998; 83:1132–1143. [PubMed: 9831708]
4. Masia R, Enkvetchakul D, Nichols CG. Differential nucleotide regulation of katp channels by sur1 and sur2a. J Mol Cell Cardiol. 2005; 39:491–501. [PubMed: 15893323]
5. Findlay I, Faivre JF. Atp-sensitive k channels in heart muscle. Spare channels. FEBS Lett. 1991; 279:95–97. [PubMed: 1995351]
6. Bao L, Kefaloyianni E, Lader J, et al. Unique properties of the atp-sensitive k(+) channel in the mouse ventricular cardiac conduction system. Circ Arrhythm Electrophysiol. 4:926–935. [PubMed: 21984445]
7. Flagg TP, Kurata HT, Masia R, et al. Differential structure of atrial and ventricular katp: Atrial katp channels require sur1. Circ Res. 2008; 103:1458–1465. [PubMed: 18974387]
8. Ripoll C, Lederer WJ, Nichols CG. Modulation of atp-sensitive k+ channel activity and contractile behavior in mammalian ventricle by the potassium channel openers cromakalim and rp49356. J Pharmacol Exp Ther. 1990; 255:429–435. [PubMed: 2243335]
9. Weiss JN, Venkatesh N, Lamp ST. Atp-sensitive k+ channels and cellular k+ loss in hypoxic and ischaemic mammalian ventricle. J Physiol. 1992; 447:649–673. [PubMed: 1593462]
10. Shaw RM, Rudy Y. Electrophysiologic effects of acute myocardial ischemia: A theoretical study of altered cell excitability and action potential duration. Cardiovasc Res. 1997; 35:256–272. [PubMed: 9349389]

11. Kane GC, Behfar A, Yamada S, et al. Atp-sensitive k+ channel knockout compromises the metabolic benefit of exercise training, resulting in cardiac deficits. Diabetes. 2004; 53(Suppl 3):S169–S175. [PubMed: 15561907]
12. Zingman LV, Hodgson DM, Bast PH, et al. Kir6.2 is required for adaptation to stress. Proc Natl Acad Sci U S A. 2002; 99:13278–13283. [PubMed: 12271142]
13. Poitry S, van Bever L, Coppex F, Roatti A, Baertschi AJ. Differential sensitivity of atrial and ventricular k(atp) channels to metabolic inhibition. Cardiovasc Res. 2003; 57:468–476. [PubMed: 12566119]
14. Nichols CG, Ripoll C, Lederer WJ. Atp-sensitive potassium channel modulation of the guinea pig ventricular action potential and contraction. Circ Res. 1991; 68:280–287. [PubMed: 1984868]
15. Decker KF, Heijman J, Silva JR, Hund TJ, Rudy Y. Properties and ionic mechanisms of action potential adaptation, restitution, and accommodation in canine epicardium. Am J Physiol Heart Circ Physiol. 2009; 296:H1017–H1026. [PubMed: 19168720]
16. Liu Y, Ren G, O'Rourke B, Marban E, Seharaseyon J. Pharmacological comparison of native mitochondrial k(atp) channels with molecularly defined surface k(atp) channels. Mol Pharmacol. 2001; 59:225–230. [PubMed: 11160857]
17. Ashcroft FM, Gribble FM. Tissue-specific effects of sulfonylureas: Lessons from studies of cloned k(atp) channels. J Diabetes Complications. 2000; 14:192–196. [PubMed: 11004427]
18. Sicouri S, Antzelevitch C. A subpopulation of cells with unique electrophysiological properties in the deep subepicardium of the canine ventricle. The m cell. Circ Res. 1991; 68:1729–1741. [PubMed: 2036721]
19. Nichols CG, Lederer WJ. The regulation of atp-sensitive k+ channel activity in intact and permeabilized rat ventricular myocytes. J Physiol. 1990; 423:91–110. [PubMed: 2388163]
20. Inagaki N, Tsuura Y, Namba N, et al. Cloning and functional characterization of a novel atp-sensitive potassium channel ubiquitously expressed in rat tissues, including pancreatic islets, pituitary, skeletal muscle, and heart. J Biol Chem. 1995; 270:5691–5694. [PubMed: 7890693]
21. Fedorov VV, Glukhov AV, Ambrosi CM, et al. Effects of k(atp) channel openers diazoxide and pinacidil in coronary-perfused atria and ventricles from failing and non-failing human hearts. J Mol Cell Cardiol. 51:215–225. [PubMed: 21586291]
22. Chan KW, Wheeler A, Csanady L. Sulfonylurea receptors type 1 and 2a randomly assemble to form heteromeric katp channels of mixed subunit composition. J Gen Physiol. 2008; 131:43–58. [PubMed: 18079561]
23. Cheng WW, Tong A, Flagg TP, Nichols CG. Random assembly of sur subunits in k(atp) channel complexes. Channels (Austin). 2008; 2:34–38. [PubMed: 18690055]
24. Zhang HX, Akrouh A, Kurata HT, et al. Hmr 1098 is not an sur isotype specific inhibitor of heterologous or sarcolemmal k atp channels. J Mol Cell Cardiol. 2011; 50:552–560. [PubMed: 21185839]
25. Flagg TP, Patton B, Masia R, et al. Arrhythmia susceptibility and premature death in transgenic mice overexpressing both sur1 and kir6.2[deltan30,k185q] in the heart. Am J Physiol Heart Circ Physiol. 2007; 293:H836–H845. [PubMed: 17449558]
26. Toib A, Zhang HX, Broekelmann TJ, et al. Cardiac specific atp-sensitive k(+) channel (k(atp)) overexpression results in embryonic lethality. J Mol Cell Cardiol. 53:437–445. [PubMed: 22796573]
27. Antzelevitch C. Modulation of transmural repolarization. Ann N Y Acad Sci. 2005; 1047:314–323. [PubMed: 16093507]
28. Furukawa T, Kimura S, Furukawa N, Bassett AL, Myerburg RJ. Role of cardiac atpregulated potassium channels in differential responses of endocardial and epicardial cells to ischemia. Circ Res. 1991; 68:1693–1702. [PubMed: 2036719]
29. Di Diego JM, Antzelevitch C. Pinacidil-induced electrical heterogeneity and extrasystolic activity in canine ventricular tissues. Does activation of atp-regulated potassium current promote phase 2 reentry? Circulation. 1993; 88:1177–1189. [PubMed: 7689041]
30. Yan GX, Antzelevitch C. Cellular basis for the brugada syndrome and other mechanisms of arrhythmogenesis associated with st-segment elevation. Circulation. 1999; 100:1660–1666. [PubMed: 10517739]

31. Kimura S, Bassett AL, Furukawa T, Furukawa N, Myerburg RJ. Differences in the effect of metabolic inhibition on action potentials and calcium currents in endocardial and epicardial cells. Circulation. 1991; 84:768–777. [PubMed: 1860220]

32. Roden DM. Repolarization reserve: A moving target. Circulation. 2008; 118:981–982. [PubMed: 18765386]

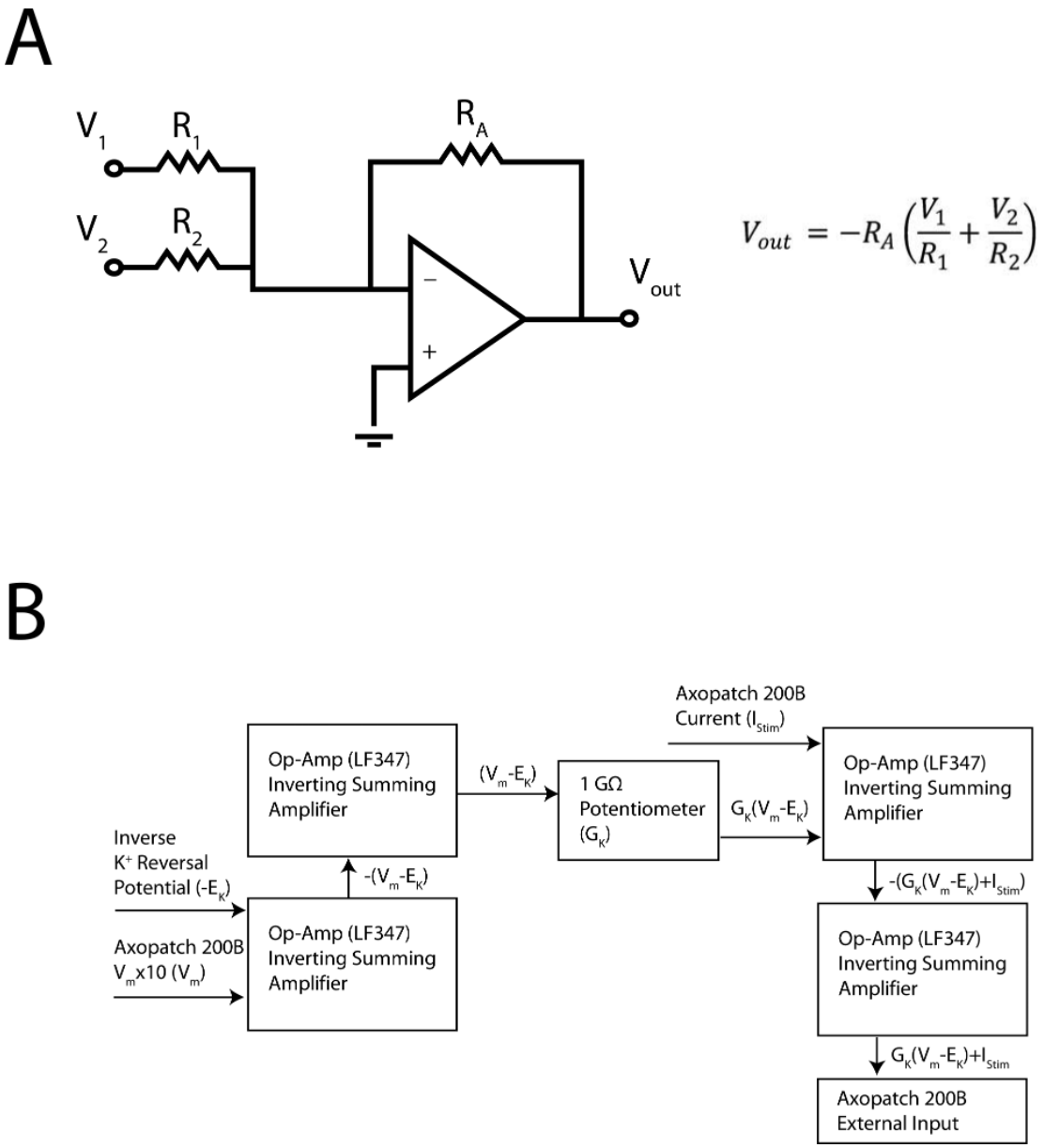

Figure 1.

Dynamic Clamp Circuit for applying $K_{ATP\text{-}INJ}$. The goal was to add the result of the following equation $I_{KATP\text{-}INJ} = G_K(V_m\text{-}E_K)$ to the stimulus, I_{Stim}. G_K is the $K_{ATP\text{-}INJ}$ conductance, V_m is the transmembrane potential measured by the amplifer and E_K is the reversal potential of K^+, –80 mV set by the D/A amplifier. (A) The circuit relied on a series of inverting operational amplifiers (A), which were combined (B) to generate the real time $K_{ATP\text{-}INJ}$ simulated conductance applied to the current-clamped cell.

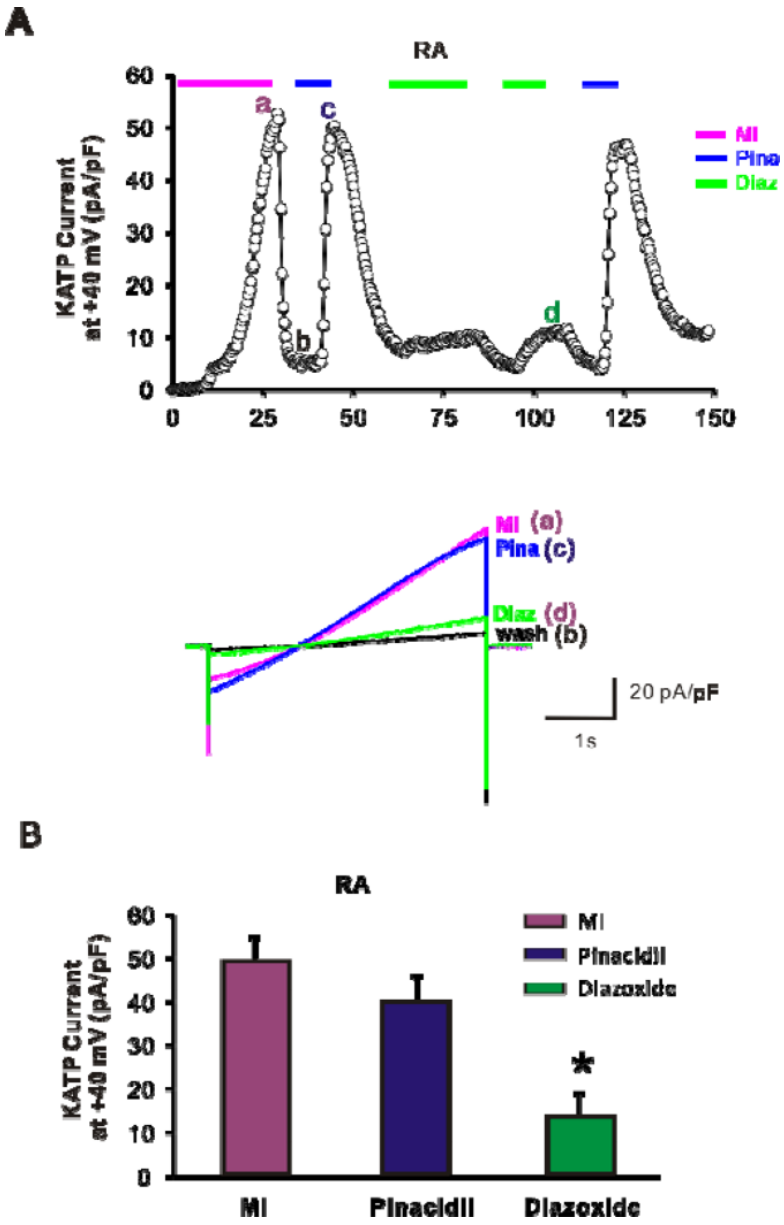

Figure 2.

Whole-cell patch-clamp recordings of K_{ATP} currents from dog atrial myocytes. (A) Time courses of whole-cell K_{ATP} currents induced by metabolic inhibition (above, MI, 10 mM deoxyglucose + 10 mM NaCN), 100 μM pinacidil, and 100 μM diazoxide from right atrial myocyte. (below) Raw traces from the time points indicated above. (B) Summary of K_{ATP} currents in dog atrial myocytes. MI and pinacidil (Pina) activate comparable currents from dog atrial myocytes.

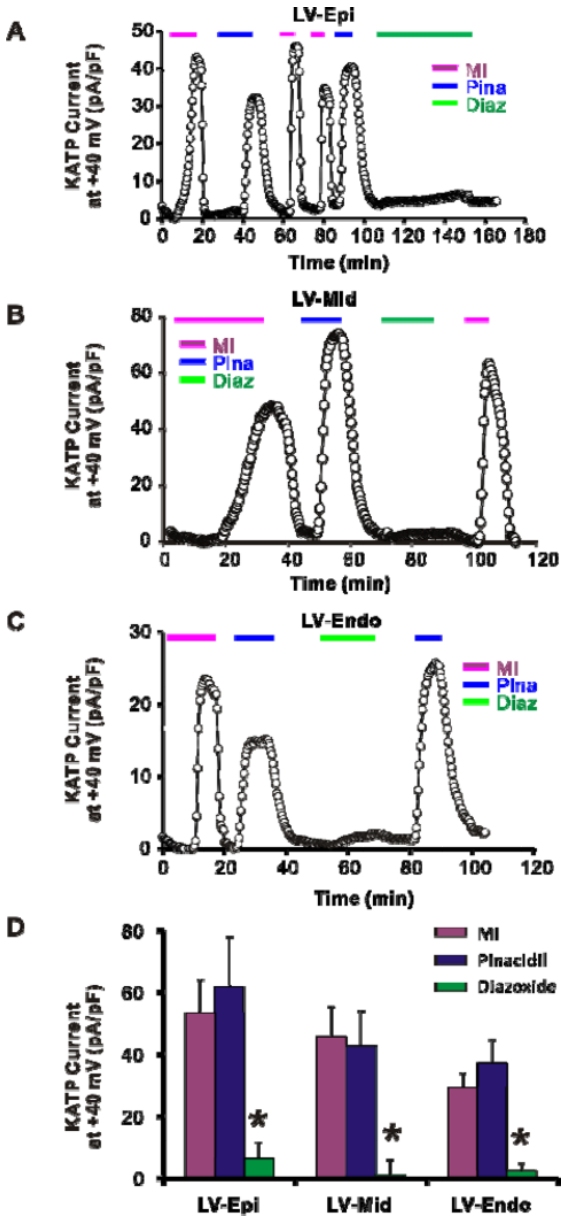

Figure 3.

Whole-cell patch-clamp recordings of K_{ATP} current from dog ventricular myocytes. Time courses of whole-cell K_{ATP} currents induced by metabolic inhibition (MI, 10 mM deoxyglucose + 2 mM NaCN), 100 μM pinacidil, and 100 μM diazoxide on dog myocytes from epicardium (Epi) (A), mid myocardium (Mid) (B), and endocardium (Endo) (C). (D) Summary of K_{ATP} currents in dog ventricular myocytes. Pinacidil activates large K_{ATP} currents from Epi, Mid, and Endo, while diazoxide induces negligible current. *p<0.05 vs MI and Pina groups in Epi, Mid or Endo two-way ANOVA followed by Bonferroni's post-tests

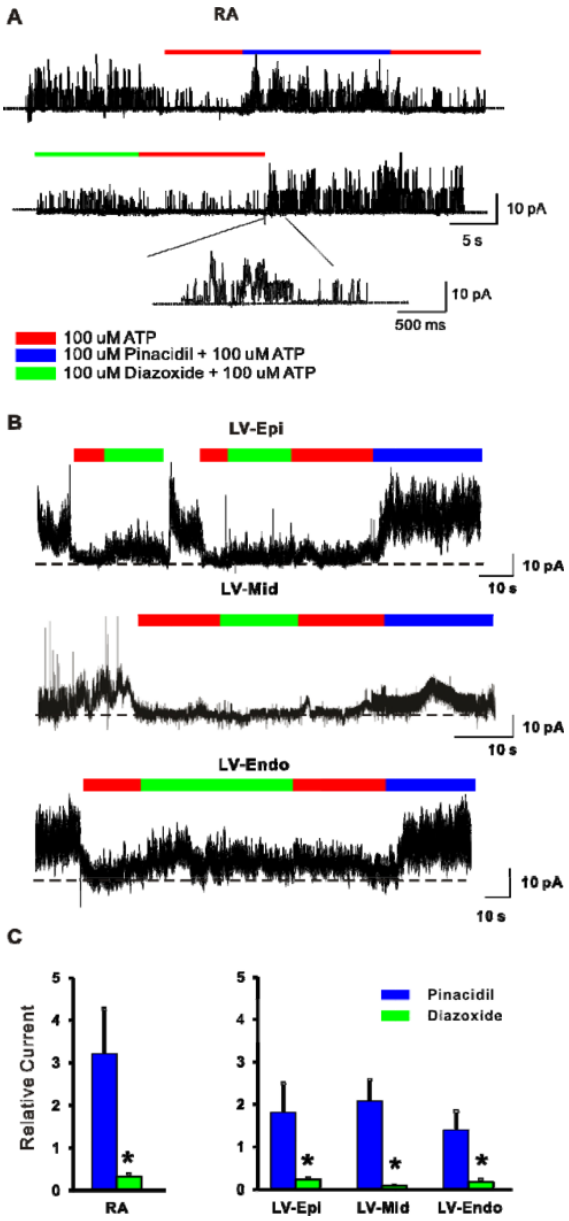

Figure 4.

Excised inside-out patch recordings of K_{ATP} currents from dog myocytes. Representative traces showing K_{ATP} current induced by 100 μM pinacidil and 100 μM diazoxide from excised inside-out patches of dog myocytes from (A) right atrium (RA), (B) ventricular epicardium (Epi, top), mid-myocardium (Mid, middle), and endocardium (Endo, bottom) . Part of recording in A is enlarged as indicated. Diazoxide- or pinacidil-induced current was normalized to ATP-free Kint current. (C) Summary of K_{ATP} patch currents from atrial (left) and ventricular (right) myocytes. Pinacidil activates larger patch currents from atrial and ventricular myocytes. *p<0.05 vs. pinacidil group two-way ANOVA followed by Bonferroni's post-tests.

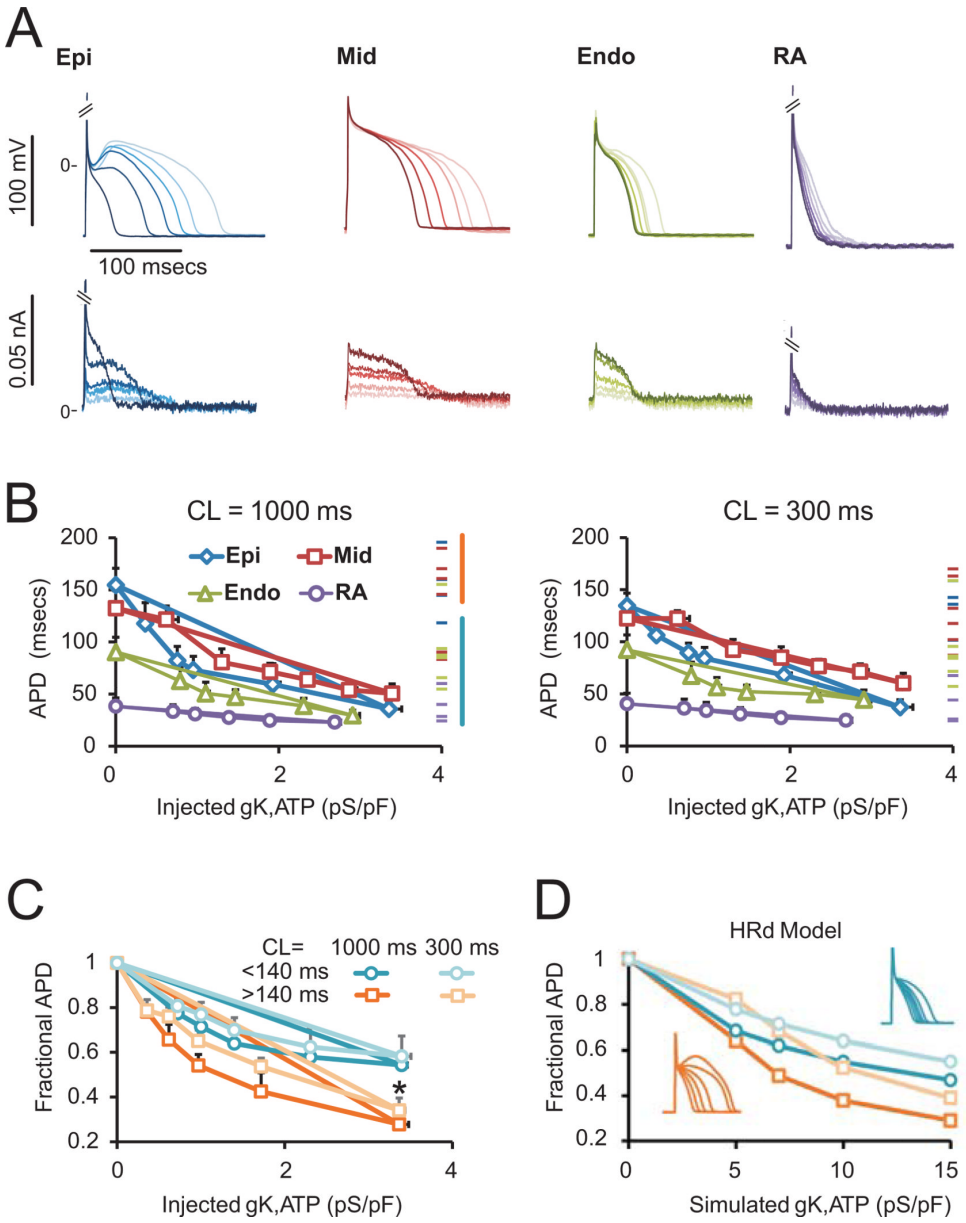

Figure 5.

Dynamic-clamp and computational simulations of K_{ATP} conductance effects on action potentials. (A) Representative traces of Epi, Mid, Endo and right atrial APs obtained with perforated patch. Injected currents via dynamic clamp are shown below. Shading of currents corresponds with shading of APs. Increasing $K_{ATP\text{-}INJ}$ results in significant APD shortening. (B) APD as a function of conductance, normalized to capacitance, at CL=1000 ms and 300 ms. Epi and mid cells (with longer APs) are more sensitive to $K_{ATP\text{-}INJ}$, an effect which is blunted as the AP becomes shorter in response to increased rate. (C) Normalizing to starting APD shows that myocytes with longer APDs undergo greater fractional shortening. *p<0.05, APD>140 ms group vs. APD<140 ms group for both CL=1000 ms and CL=300

ms by a two-tailed student t-test. (D) APs simulated with the HRd canine ventricular model (insets show APDs with increasing K_{ATP}).